



CNN-based Approach for Enhancing Brain Tumor Image Classification Accuracy

A. Muis^a, S. Sunardi^{*b}, A. Yudhana^b

^a Graduate Program of Informatics, Universitas Ahmad Dahlan, Indonesia

^b Department of Electrical Engineering, Universitas Ahmad Dahlan, Indonesia

PAPER INFO

Paper history:

Received 29 October 2023

Received in revised form 13 December 2023

Accepted 28 December 2023

Keywords:

Accuracy

Brain Tumor

Convolutional Neural Network

Machine Learning

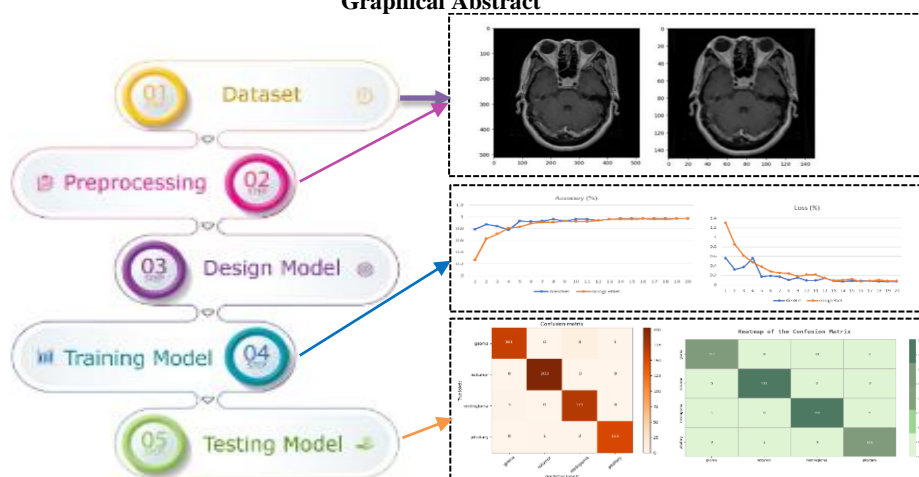
Magnetic Resonance Image

ABSTRACT

Brain tumors are one of the deadliest diseases in the world. This disease can attack anyone regardless of gender or certain age groups. The diagnosis of brain tumors is carried out by manually identifying images resulting from Computerized Tomography Scan or Magnetic Resonance Imaging, making it possible for diagnostic errors to occur. In addition, diagnosis can be made using biopsy techniques. This technique is very accurate but takes a long time, around 10 to 15 days and involves a lot of equipment and medical personnel. Based on this, machine learning technology is needed which can classify based on images produced from MRI. This research aims to increase the accuracy of previous research in the classification of brain tumors so that errors do not occur in the diagnosis of brain tumors. The method used in this research is Convolutional Neural Network using the AlexNet and Google Net architectures. The results of this research obtained an accuracy of 98% for the AlexNet architecture and 96% for GoogleNet. This result is higher when compared with previous research. This finding can reduce the computational burden during model training. The results of this research can help physicians diagnose brain tumors quickly and accurately.

doi: 10.5829/ije.2024.37.05b.15

Graphical Abstract



1. INTRODUCTION

Brain tumors are considered one of the most dreaded diseases by humans. It is a life-threatening condition that can occur in individuals regardless of age, gender, or

specific groups (1). Essentially, brain tumors can grow and develop in parts of the body surrounding the brain (2). Brain tumors are characterized by the uncontrolled growth of cells, which continue to proliferate in the affected area of the body. This excessive cell growth is

*Corresponding Author Email: sunardi@mti.uad.ac.id (S. Sunardi)

unnecessary for the body or any specific organ. Instead, it disrupts the body's metabolism and can impair the function of nearby organs surrounding the tumor (3). Brain tumors are tumors that develop and grow in the vicinity of the skull. Based on their growth characteristics, brain tumors can be classified into two types benign brain tumors and malignant brain tumors. Benign brain tumors have a slow growth rate and do not spread to surrounding tissues, but they can still damage the brain. On the other hand, malignant tumors exhibit rapid growth and can invade surrounding tissues. Brain tumors are considered one of the most dangerous diseases in the world. This disease is one of the deadliest diseases, posing a significant threat to individuals affected by them (4). Only about one third of patients with this disease survive for five years after diagnosis.

Doctors diagnose brain tumors in patients using several methods. First, they assess the patient's physical condition and medical history, including examining the neural tissues within the skull to determine if they are intact or compromised. Second, they employ scanning machines such as CT Scan and Magnetic Resonance Imaging (MRI) to aid in the diagnosis (5). CT Scan is performed using X-ray machines to provide doctors with a clearer view of the patient's condition, including body structures and blood cells. On the other hand, MRI differs from CT Scan as it does not involve radiation and can generate clear images of the skull, allowing for diagnosis based on the MRI scan results. MRI scans produce detailed images of the body's organs using a magnetic field, but this technique often requires a longer duration (6, 7). The third method is the collection of body tissues for examination by a neuropathologist. This technique is called a biopsy. Biopsy can also assist doctors in diagnosing the type of brain tumor, whether it is benign or malignant, present in the patient. The biopsy process can indeed be time-consuming as the collected tissue samples need to be sent to the laboratory for examination. However, it is crucial to diagnose this disease quickly and accurately to ensure appropriate treatment. Therefore, early detection technology is needed for brain tumor diagnosis in patients. Additionally, monitoring the progression of brain tumors in affected patients is essential for effective management of the disease (8). Machine learning techniques can indeed be utilized to detect brain tumors by leveraging brain images obtained from MRI scans. This highlights the significant impact of machine learning development in the field of healthcare, enabling effective detection and classification of specific diseases, including brain tumors (9-12). The aim is to facilitate prompt and accurate treatment or therapy for patients diagnosed with brain tumors, considering that the treatment process can be lengthy (13).

Machine learning is a branch of Artificial Intelligence (AI) that involves designing and developing algorithms with the goal of enabling computers to learn from data

provided to them. The data can be in the form of binary data, images, videos, or even sound, and can be learned by the technology. machine learning can also recognize handwriting (14). This capability assists humans in solving image processing problems. Image processing is highly valuable in the field of healthcare as it aids in detecting diseases within the human body by utilizing medical images generated from CT or MRI scans. The classification of medical images using deep learning is an important research topic because it has broad applications in the diagnosis of various diseases (15-19). Images from MRI scans are extracted to generate new image data based on created algorithms. The most commonly used algorithm for image extraction and classification using deep learning is Convolutional Neural Network (CNN) (20, 21).

CNN has emerged as the leading algorithm for performing classification of medical images in recent years (22-25). CNN is capable of efficiently classifying a large number of images (26). Essentially, the CNN algorithm consists of two main stages in the classification process following the input of an image feature extraction and classification. CNN can decrease the count of trainable network parameters by leveraging a blend of characteristics sourced from multiple layers to enhance the overall accuracy (27). The feature extraction stage comprises convolutional layers and pooling, while the classification stage involves fully connected layers and the output layer (28). Figure 1 is a general feature extraction stage in CNN.

Figure 1 shows that the input image measuring 150x150 is convolved using a 3x3 kernel with ReLU activation and using Maxpooling size 2x2. The convolutional layer is a crucial component of the CNN algorithm as it generates new images after convolving the input image. This process involves applying filters to extract features from the input image. The filters used are typically matrices of sizes 1x1, 3x3, 5x5, or 7x7. The filter operation produces a feature map by altering the values of each feature map. After the feature map is obtained, pooling is performed. Pooling is not conducted until the convolutional layer generates a new feature map from the input image. Pooling is a process of reducing the size of the image while retaining important information. The commonly used pooling layers are max pooling and average pooling. Max pooling involves selecting the highest value within each filter to generate a new image,

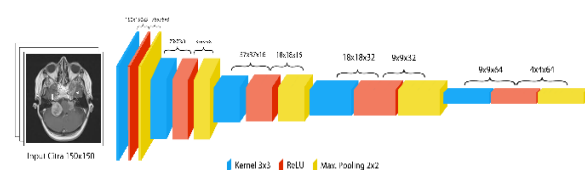


Figure 1. CNN Algorithm

while average pooling calculates the average value of each matrix passed through the filter. The pooling filter size is often 2x2. The output obtained from pooling is converted into a vector and fed into the fully connected layer, which is the last layer in the CNN algorithm. The layers from the previous stage are connected to the neurons in the subsequent layer, similar to a typical artificial neural network (11). In this layer, activation functions such as sigmoid or softmax are used to determine the classification of the image displayed in the output. The output represents the result of the fully connected layer, where it classifies the input image into specific labels or classes. The output assigns the input image to its corresponding class based on the similarity or similarity to the learned data.

CNN has gained popularity as a powerful algorithm for classifying images in various domains, including medical imaging. Whether it's brain images or other types of medical images, CNN has demonstrated its effectiveness in accurately classifying and analyzing them (29). Its ability to learn and capture intricate patterns in images has made it a popular choice for image classification tasks in the field of medical technology.

Ismael and Abdel-Qader (30) conducted a study to classify brain tumor diseases using a neural network. This research utilized brain tumor images obtained from MRI scans. The dataset employed in the study consisted of 3064 samples, including three classes: glioma, meningioma, and pituitary. Figure 2 in the study reveals that the classification technique employed a multilayer neural network comprising three layers: input, hidden, and output. The input layer consisted of 270 neurons, one hidden layer contained 90 neurons, and the output layer comprised 3 neurons. The study achieved an accuracy of 96% for the meningioma class, 96.29% for glioma, and 95.66% for pituitary, resulting in an overall accuracy of 91.9%. The study conducted by Pashaei et al. (23) examined the CNN and Extreme Learning Machines (ELM) methods for brain tumor classification. This research utilized MRI images of meningioma, glioma, and pituitary tumors, with a total dataset of 3064 samples. The study employed 4 convolutional layers, 4 pooling layers, and 1 fully connected layer. They presented the results of the confusion matrix analysis to determine the precision, recall, and F-measure values using the CNN algorithm, where the pituitary class achieved the highest percentages of 98.3%, 100%, and 99.1% respectively. The study yielded the highest accuracy of 93.68% using CNN [23]. Anaraki et al. (31) conducted a study on the classification of MRI images using neural networks and the Genetic algorithm. The dataset used in this research consisted of 600 brain tumor images, classified into three classes: glioma, meningioma, and pituitary. In their study illustrated the implementation of CNN architecture, which includes two case studies. In the first case study, 4x4 convolutional layer was used, followed by max

pooling with size of 2x2. The final convolutional layer had a size of 6x6, resulting in a total of 96 feature maps for case study one. In the second case study, a 6x6 convolutional layer was used, along with max pooling of size 2x2. The final convolutional layer had size of 4x4, generating 384 feature maps. The study achieved an accuracy of 94.2% (31). These results demonstrate that the employed methods are highly effective in classifying brain tumors based on MRI images. Baranwal et al. conducted a performance analysis of the classification methods CNN and Support Vector Machine (SVM) using brain MRI images. The aim of this study was to classify brain tumor diseases, including meningioma, glioma, and pituitary tumors. Figure 3 in the study presents a CNN architecture, consisting of 5 convolutional layers with max pooling. Each image resulted in 1024 feature maps, which were classified into their respective classes. The classification results were analyzed to determine the best method for classification. The study achieved an accuracy of 94% using the CNN algorithm and 81% using SVM (32). These results demonstrate that CNN is more effective and accurate compared to the SVM algorithm. The classification conducted by Deepak et al. focused on common brain tumors, namely glioma, meningioma, and pituitary tumors. The research method employed CNN with the GoogLeNet architecture. In their study presented a comparison with previous similar research studies. The conclusion drawn after comparing the results with prior studies indicates that the algorithm used in this research outperforms the previous findings in terms of accuracy. The study achieved a high accuracy of 98% (33). Research on brain tumors with the highest accuracy of 98.76% was obtained using the ResNet algorithm, but this research used data on 233 brain tumor patients plus 980 without brain tumors (34). In addition, edge detection of images affected by brain tumors has been carried out, but still obtains low accuracy, namely 86.59% (35). Edge detection is the most important part in knowing where the tumor is. Research using the AlexNet and GoogLeNet architectures carried out previously obtained an accuracy of 95.77% for the AlexNet-Conv5 architecture and 95.44 for GoogLeNet-inception-4e (36). This research has differences with the model proposed in this research. that research uses the original input image while this research reduces the input image to reduce the computational load.

Previous research studies have often utilized the CNN algorithm for image classification, as CNN has shown success in solving classification problems (37). The images used in these studies are brain images obtained from MRI scans, including both images with brain tumors and images without brain tumors. Several studies have achieved high accuracy in classifying brain tumor images.

This research aims to improve the accuracy of previous studies by utilizing advanced CNN-based

algorithms that have been developed (38). The technique used in this research starts by changing the input image to a smaller size. The input image is tested using the AlexNet and GoogLeNet algorithms. Before testing, the dataset is divided into test data and testing data. Test data is further divided into test data and validation data. This aims to test the model during the training process. During the training process, the Callback function used is ReduceLRonPlateau. The function helps adjust the learning rate used so that the training process is stable and prevents overfitting. Next, testing is carried out using testing data to produce a confusion matrix which is analyzed to determine the level of accuracy obtained.

2. METHOD

The research methodology begins with the collection of brain tumor data obtained from MRI scans. The dataset then undergoes a preprocessing stage to clean and organize the data. Following that, a model is designed for classifying the dataset. Before conducting the classification, the created model undergoes training using a training dataset to improve its performance. Once the model is trained, it is then tested using a separate dataset to evaluate its classification capabilities. This process aims to assess the model's ability to accurately classify new datasets. Figure 2 illustrated the proposed research methods.

Figure 2 is the proposed method which starts from the search stage for brain tumor image datasets, the data preparation stage to be used as training and testing data, the model design stage according to the proposed model, the model training stage using training data, the model testing stage to test the proposed model.

2.1. Datasets Dataset is a collection of data that can be in the form of numbers, images, or other formats, containing information relevant to the research. In this particular study, the dataset consists of brain images obtained from MRI scans, as MRI images are well-suited



Figure 2. Research method

for extracting image features using CNN (32). The MRI brain images downloaded for this study are categorized into four classes: glioma tumor, meningioma tumor, no tumor, and pituitary tumor. The dataset used in this research includes 7023 brain images, which are divided into 6320 for training the model and 703 for testing the model.

2.2. Preprocessing Preprocessing is a stage of preparing the dataset so that the data can be processed by machine learning architectures (39). Preprocessing the data can also enhance the performance of the application in extracting features from images (40). The preprocessing techniques used in this research include resizing and grayscale conversion. Resizing is the process of adjusting the size of input images to a uniform size before classification using the CNN algorithm.

Based on Figure 3, it is observed that the images before preprocessing have a size of 500x500. This large image size can pose challenges for the model in performing classification as it requires more time to extract image features (41). Therefore, resizing is performed to ensure that the dataset used has consistent size. In this research pixel size of 150x150 is used. Although the image size used is significantly different from the original size, it does not compromise the image information. Grayscale is the process of converting the color image to grayscale image. The brain images used in this research consist of three color channels (RGB), hence grayscale is performed to convert the three channel image into two channel image, enabling better classification by the employed architecture.

2.3. Design Model This stage involves the creation of a model or architecture for classifying the dataset. In this research, two CNN architectures, namely AlexNet and GoogLeNet, are utilized. AlexNet is a neural network architecture developed by Alex Krizhevsky. The AlexNet input image size that we proposed is 150x150. This size is different from the original AlexNet input image size, which is 227x227 with three different filters. This size is extracted in the convolution layer until it reaches a fully connected layer with a number of

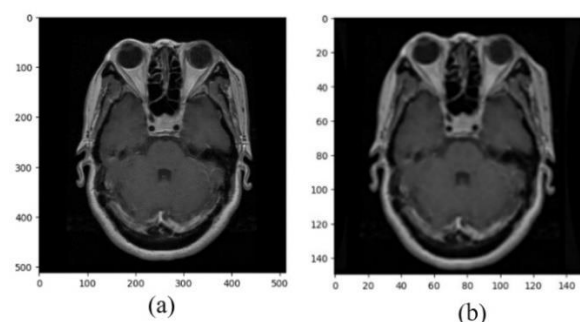


Figure 3. Preprocessing image (a) before (b) after

parameters 2304. The output results are different from the output results in the original AlexNet architecture, namely 9216 parameters. This difference is due to the input size of the image used, namely 150x150. Next, a fully connected layer with 4096 parameters is added until it is activated using the softmax function with four class output. Both architectures were developed to participate in the ImageNet LSVRC-2010 competition, which involved classifying images with a large number of classes. AlexNet emerged as the winner in 2012, while GoogLeNet claimed the top spot in 2014, surpassing AlexNet's performance. In this research, both architectures are employed to enhance the accuracy of classifying brain images from MRI scans.

The CNN architecture is a deep learning architecture in machine learning that consists of feature extraction and fully connected layers (42). In the feature extraction stage, there are several layers that are responsible for extracting features from images, transforming them into new images known as feature maps. The fundamental steps in feature extraction are the convolution and pooling layers. Convolution involves the multiplication of two matrices followed by summation.

Equation to calculate convolution in the feature extraction stage of CNN architecture is stated as follows.

$$C(i,j)=\sum_m\sum_n I(i+m,j+n) \cdot K(m,n) \tag{1}$$

The value of C(i,j) represents the convolution result at pixel location (i,j) in the feature map. I(i+m,j+n) denotes the pixel value in the input image at location (i+m,j+n), K(m,n) represents the value in the convolution kernel at location (m,n), and $\sum_m\sum_n$ indicates the summation operation over variables m and n according to the kernel size. Furthermore, the convolutional results can pass through activation functions such as ReLU (Rectified Linear Unit) to introduce non-linearity to the extracted features. After the convolutional stage, a pooling layer is applied, which aims to reduce the spatial dimensions of the feature map while preserving important information. One commonly used type of pooling is max pooling, where the maximum value within each pooling window is retained. The feature extraction process in CNN architecture is repeated with multiple convolutional and pooling layers to generate increasingly complex and abstract features from the input image.

Another equation that can be used to calculate convolution is as follows.

$$a \cdot b = \sum_{i=1}^n a_i b_i = a_1 b_1 + a_2 b_2 + \dots + a_n b_n \tag{2}$$

The values of a and b represent the values in the kernel used, with a kernel size of 2x2. If using a 3x3 kernel, the kernel values will not only include a and b but also an additional value, c. An example implementation of Equation 1 using a 2x2 kernel, a 3x3 image size, employing zero padding, stride 1, and the following

values for the kernel: a1=1, a2=2, b1=3, and b2=4 as in Figure 4.

Figure 4 show values in the kernel are multiplied by the values in the 2x2 image matrix, resulting in a1=0, a2=0, b1=0, and b2=4. Therefore, the sum of these values is 4. Consequently, the initial value in the feature map matrix is 4. This operation is performed until the entire matrix has been traversed by the kernel.

The convolutional stage produces new images or feature maps derived from overlapping pixels of the input image, resulting in multiple feature maps when the input image is convolved multiple times. The feature map generated for each image can be calculated using the following equation.

$$n_{out} = \left\lfloor \frac{n_{in} + 2p - k}{s} \right\rfloor + 1 \tag{3}$$

The value of n_out represents the resulting feature map size after each convolution operation, n_in represents the input layer size or the size of the image being used, p represents the padding size applied, k represents the size of the kernel used, and S represents the stride value, indicating the movement of the kernel both horizontally and vertically. In this study, the feature maps generated after each convolution operation can be calculated. The study utilizes input images of size 150x150, applies zero padding, uses a 3x3 filter size, and employs a stride of one for kernel movement.

The resulting new features from one convolutional step are as follows.

$$n_{out} = \left\lfloor \frac{150 + 2 \times 1 - 3}{1} \right\rfloor + 1$$

Based on that, the resulting feature map will have the same size as the input image, which is 150 pixels. This is because of the use of zero padding. To determine important information within the image, one can create a histogram of the image. An image histogram is a graph that represents the distribution of pixel values in an image. The histogram can reveal a lot about the brightness and contrast of an image. Therefore, the histogram is a valuable tool for both qualitative and quantitative image processing. Mathematically, the image histogram can be calculated using the following equation.

$$h_i = \frac{n_i}{n} \tag{4}$$

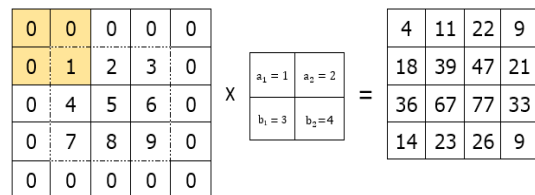


Figure 4. Convolutional layer

The value of n_i represents the number of pixels that have a certain gray level in the image, while n represents the total number of pixels in the image. As an example, Figure 5 displays the binary extraction result of brain tumor images, represented in matrix form.

Figure 5 displays the result of image extraction in the form of a binary data matrix that can be used to generate a histogram. Figure 5 shows an image with a size of 150x150, which means that the value of n is 22,500 pixels. To determine the value of n_i the number of occurrences of each binary data needs to be known. Figure 6 represents the histogram generated from processing the binary data of brain tumor images.

The difference in the proposed architectural model lies in the use of the input image size which uses a size of 150x150 for AlexNet and GoogLeNet respectively. The actual input image size of AlexNet is 227x227 while GoogLeNet is 224x224. The size of 150x150 is proposed because it will reduce the computational load and the model training process is relatively fast.

2. 4. Training Model A training dataset for image in machine learning is a collection of image data used to train models or algorithms to learn visual patterns. This dataset plays a crucial role in tasks such as image recognition, object detection, segmentation, and various other image processing tasks. Essentially, each image in

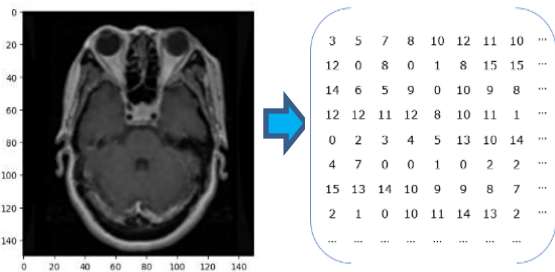


Figure 5. Binary data of brain image

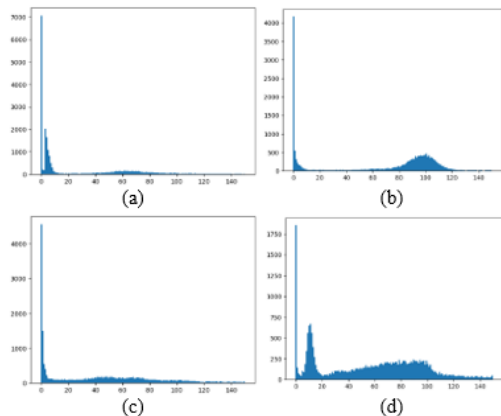


Figure 6. Histogram image (a) glioma (b) notumor (c) meningioma (d) pituitary

the training dataset is considered as an input consisting of a pixel matrix that represents the light intensity at each point in the image. The pixel values are typically represented on a scale of 0-255, where 0 represents the color black and 255 represents the color white. In addition, labels or annotations are also an integral part of a training dataset for images. These labels serve to provide information about the class or category represented by each image in the dataset. For example, in a face recognition dataset, each image would be assigned a label indicating the identity of the person depicted in the image. These labels are necessary to train the model to recognize and differentiate between different objects or classes. In the context of this study, the labels represent the classes of the dataset, which include glioma, notumor, meningioma, and pituitary.

The training of the model is an essential step in the experimentation process before conducting model testing. The initially created model may not classify images accurately since it hasn't learned from the dataset. Therefore, the training phase is crucial as the model needs to learn to recognize patterns in the given dataset (43). The model is first trained using the training data, which consists of 6,320 (90%) images out of the total 7,023 brain MRI dataset. This allows the model to learn from the provided dataset. Before training, the training data is divided into 32 batches (batch size). The training process is carried out for 20 iterations (epochs). Each model used in this research is trained with a scenario of batch size 32, 20 epochs, a learning rate of 0.001, and the Adam optimization algorithm, which is known to perform better than other optimization algorithms (31).

2. 5. Testing Model This stage is performed after the model is trained using the training data. The purpose of this stage is to test the created model's ability to classify brain images using data that the model has never seen before. The testing data consists of 703 (10%) images from the total 7,023 brain MRI dataset. The results of the testing phase using the testing data are presented in the form of a confusion matrix for further analysis. A confusion matrix is a tool that displays and compares the actual values or ground truth values with the predicted values generated by the model. The results from the confusion matrix can be used to calculate evaluation metrics such as precision, recall, and F1-score. Additionally, the confusion matrix allows for the calculation of the accuracy of each model.

Figure 7 displays the confusion matrix obtained from the model testing. The confusion matrix includes the values TP (True Positive), TN (True Negative), FP (False Positive), and FN (False Negative). TP represents the correctly predicted data for each class. For example, the TP value for the glioma class is A1, for the meningioma class is B2, for the notumor class is C3, and for the pituitary class is D4. TN is the sum of all values in the

| | | | |
|----|----|----|----|
| A1 | A2 | A3 | A4 |
| B1 | B2 | B3 | B4 |
| C1 | C2 | C3 | C4 |
| D1 | D2 | D3 | D4 |

Figure 7. Confusion matrix

matrix excluding the values from the corresponding row and column of the class. For example, the TN value for the glioma class includes B2, B3, B4, C2, C3, C4, D2, D3, and D4. FP is the sum of each column in the class excluding the TP values. For example, the FP value for the glioma class includes B1, C1, and D1. FN is the sum of each row excluding the TP values. For example, the FN value for the glioma class includes A2, A3, and A4. The obtained results from the confusion matrix are processed to calculate the accuracy percentage for each model created. The processing of the confusion matrix results is performed using the following equation (44, 45).

$$Precision = \frac{TP}{TP+FP} \quad (5)$$

$$Recall = \frac{TP}{TP+FN} \quad (6)$$

$$F1 - Score = 2 \times \frac{Precision \times Recall}{Precision + Recall} \quad (7)$$

$$Accuracy = \frac{\sum TP}{Total Data} \quad (8)$$

Precision is the ratio of TP (True Positive) to the total number of data predicted as positive. A smaller value of FP (False Positive) will increase the precision value. Recall is the ratio of TP to the total number of data actually positive. A smaller value of FN (False Negative) will increase the recall value. F1-Score is the harmonic mean of precision and recall. The best F1-Score value is 1.0, and the worst value is 0. Accuracy measures the correctness of the predicted values compared to the true values. Model testing uses accuracy to evaluate the performance of a model in classification. Each model used in this study was tested using the same testing scenario. After going through all the aforementioned steps, the next step is to examine the best test results based on the accuracy percentage of each model used in classifying brain tumor images based on their labels.

Additionally, attention is also given to the training time required based on the number of iterations performed.

3. RESULT AND DISCUSSION

This study was conducted by reviewing several previous research papers. Some of the studies found related to this research achieved high accuracy, with an average accuracy above 90% (23, 28-30). This presents a challenge in conducting research to improve the accuracy using the same method (CNN) and the same object of study (brain tumor images).

3. 1. Result This research was conducted using the same dataset, which is the dataset of human brain MRI scans, to perform classification using two different architectures. Although this study employs the same method, the difference lies in the feature extraction stage, where the feature extraction is performed using the AlexNet and GoogLeNet architectures. Prior to inputting the images into these architectures, the data undergoes preprocessing to ensure consistency with other datasets. The research yields two main results: the training model results and the testing model results.

3. 1. 1. Training Model The training process is carried out using the Adam optimization, which assists the model in training. Adam aims to iteratively update the weights based on the training data. Adam optimization is a method that computes different learning rates for each parameter. In this research, the dataset consists of 7023 brain image data, which would require a significant amount of time if all the data were trained together due to the limitations of computer memory. To address this, parameters such as Batch Size and Epoch are utilized. Batch Size is a parameter used to divide the dataset into smaller groups, allowing the computer to process them one by one and update the obtained values at the end of each training data. The batch size value used in this study is 32, meaning the model will train on 32 groups of data and update the obtained values at the end of training.

The model training is performed iteratively to allow the model to learn the data accurately, as the previously learned data is revisited. Misclassifications or erroneous classifications of brain image datasets during the initial training process are learned again, enabling the second training to be correct. This helps reduce the model's errors in performing classification tasks. The model training process is conducted with 20 epochs, where each model undergoes 20 iterations. There is another parameter used in this study, called ReduceLRonPlateau, which reduces the learning rate if the model fails to show progress in learning based on the current learning rate during an epoch. After the completion of model training,

the results of each model experiment are saved in the .h5 format for future use in training. The training results of the dataset using the AlexNet and GoogLeNet architectures can be seen in Table 1.

Table 1 shows the results of the training data with 20 iterations. The first iteration of the AlexNet model took 111 seconds and achieved an accuracy of 0.79 with a loss of 0.56. This result is relatively low because the model is initially learning from new data, so subsequent iterations are needed to further improve its learning. On the other hand, the GoogLeNet model achieved an accuracy of 0.27 and a loss of 1.3 in the first iteration, taking a total of 156 seconds. This result is lower compared to the first iteration of the AlexNet model.

In the second iteration, there is an improvement in accuracy for both models, accompanied by a decrease in the training time. The AlexNet model achieved an accuracy of 0.87 and a loss of 0.32. This demonstrates that AlexNet is capable of improving accuracy, reducing loss values, and reducing the time required for iterations. On the other hand, the GoogLeNet model achieved an accuracy of 0.63 and a loss of 0.85. This indicates a significant increase in accuracy from 0.27 in the first iteration to 0.63 in the second iteration. Moreover, there

TABLE 1. Training result

| Epoch | AlexNet | | GoogLeNet | |
|-------|---------|----------|-----------|----------|
| | Loss | Accuracy | Loss | Accuracy |
| 1 | 0.56 | 0.79 | 1.3 | 0.27 |
| 2 | 0.32 | 0.87 | 0.85 | 0.63 |
| 3 | 0.37 | 0.84 | 0.61 | 0.71 |
| 4 | 0.56 | 0.78 | 0.47 | 0.81 |
| 5 | 0.17 | 0.93 | 0.38 | 0.83 |
| 6 | 0.19 | 0.92 | 0.28 | 0.89 |
| 7 | 0.17 | 0.93 | 0.25 | 0.91 |
| 8 | 0.1 | 0.96 | 0.24 | 0.91 |
| 9 | 0.15 | 0.93 | 0.18 | 0.93 |
| 10 | 0.09 | 0.96 | 0.21 | 0.92 |
| 11 | 0.09 | 0.96 | 0.21 | 0.92 |
| 12 | 0.14 | 0.94 | 0.14 | 0.94 |
| 13 | 0.08 | 0.96 | 0.09 | 0.96 |
| 14 | 0.07 | 0.97 | 0.1 | 0.96 |
| 15 | 0.08 | 0.97 | 0.12 | 0.96 |
| 16 | 0.08 | 0.97 | 0.07 | 0.97 |
| 17 | 0.08 | 0.97 | 0.08 | 0.96 |
| 18 | 0.07 | 0.97 | 0.1 | 0.96 |
| 19 | 0.07 | 0.97 | 0.08 | 0.97 |
| 20 | 0.07 | 0.97 | 0.08 | 0.97 |

was a significant decrease in the loss value from 1.3 to 0.27. The training time also decreased in the second iteration, with 111 seconds decreasing to 110 seconds for the AlexNet model and 156 seconds decreasing to 148 seconds for the GoogLeNet model. Figure 8 represents the accuracy graph of the training results for the dataset using the AlexNet and GoogLeNet models.

Figure 8 shows that the average results obtained initially had low values, but there was an improvement in accuracy in subsequent iterations. This indicates that both models are capable of learning the data effectively, and as the iterations progress, the accuracy increases. This improvement in accuracy also influences the loss values obtained. Figure 9 represents the graph of the loss values obtained during the training process.

Figure 9 illustrates a decreasing trend in the loss value with each iteration. This indicates that the models are able to reduce errors and learn the brain tumor dataset effectively. The decreasing loss values signify that the models are improving their ability to make accurate predictions and minimize the discrepancy between predicted and actual values in the dataset.

3.1.2. Testing Model The dataset used for training consists of 90% of the data, while 10% is used for testing the model. The purpose of testing the model is to determine its accuracy or performance. The model that was trained on the training data is used again for testing

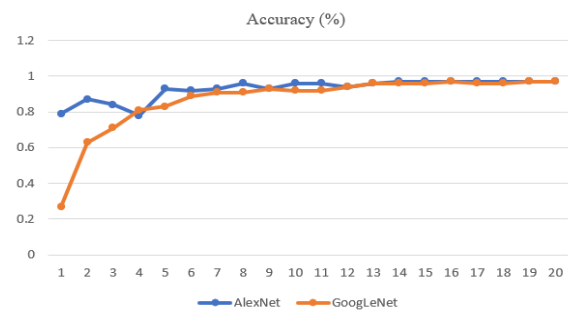


Figure 8. Accuracy training result

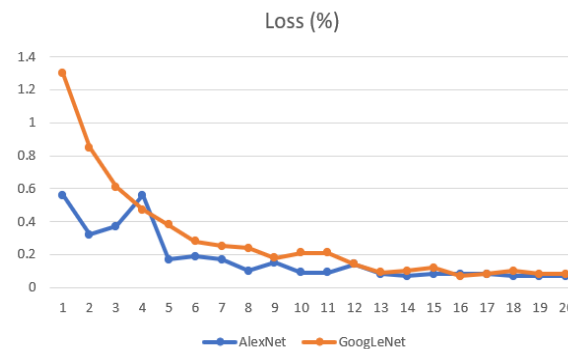


Figure 9. Loss training result

by providing a dataset that has not been previously seen by the model. This allows the model to classify the data according to what it has learned before. The results are visualized in the form of a confusion matrix, which consists of correctly classified and misclassified data for each image class. A total of 703 images are used, including 170 images of the glioma class, 203 images of the non-tumor class, 174 images of the meningioma class, and 156 images of the pituitary class. Figures 10 and 11 show the classification results visualized in the form of a confusion matrix for both the AlexNet and GoogLeNet models.

Figure 10 represents the classification results using the AlexNet model. Based on Figure 7, it is visualized in Table 2.

Table 2 shows that the highest classification result is achieved in the notumor class, where 100% of the images are correctly classified according to their classes. On the other hand, the lowest accuracy is obtained in the glioma class, with an accuracy of 95%. Despite being the lowest, this accuracy is still considered very high. The data from the confusion matrix is used in the accuracy formula to calculate the accuracy percentage. The confusion matrix resulting from the testing of the model using AlexNet achieved an accuracy of 98%, indicating that 688 images were correctly classified according to their respective classes. However, there were 15 misclassified images, accounting for a 2% error rate.

The GoogLeNet algorithm performed classification using a 10% subset of the total dataset, similar to how the dataset was used for testing the AlexNet model. One of the methods employed in GoogLeNet was image reduction, which aimed to reduce the input images while preserving crucial information. Figure 11 displays the confusion matrix obtained from evaluating the GoogLeNet model. The confusion matrix provides a visual representation of the classification results for each class. The analysis of the confusion matrix reveals the

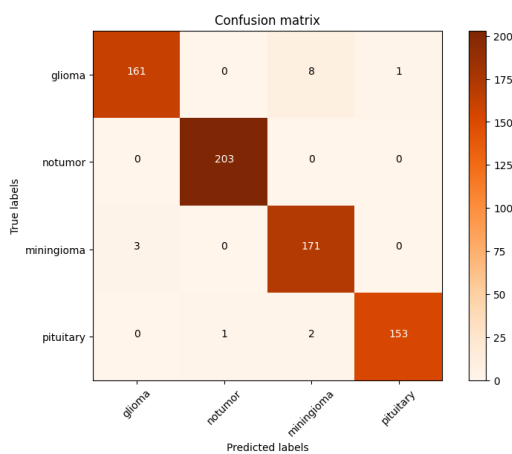


Figure 10. Confusion matrix result using AlexNet architecture

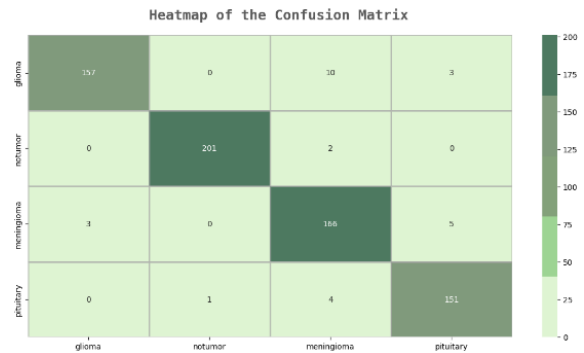


Figure 11. Confusion matrix result using GoogLeNet

TABLE 2. Classification result using AlexNet architecture

| Class | Classification True | Dataset size | Accuracy (%) |
|------------|---------------------|--------------|--------------|
| Glioma | 161 | 170 | 95 |
| Notumor | 203 | 203 | 100 |
| Meningioma | 171 | 174 | 98 |
| Pituitary | 153 | 156 | 98 |

performance of the GoogLeNet model in classifying the images.

Figure 11 displays the confusion matrix obtained from testing the pre-trained GoogLeNet architecture using a dataset of 6,335 images. The model was evaluated using a set of 703 images. The results of the testing, as shown in the confusion matrix, are visualized in Table 3.

Table 3 shows that the highest accuracy in the testing results is achieved in the "notumor" class, with a percentage of 99%. Out of a total of 203 "notumor" images, 201 of them were correctly classified. To examine the misclassified data, we can refer to the confusion matrix in Figure 11. The confusion matrix reveals that 2 misclassified data points in the "notumor" class were incorrectly classified as "meningioma". On the other hand, the lowest percentage is observed in the "glioma" class, where 157 out of 170 total "glioma" images were correctly classified. Although the accuracy is the lowest among the four classes in the dataset, it still achieves a high accuracy rate of 92%. Based on these results, the testing of the GoogLeNet architecture yields an accuracy percentage of 96%, with a total of 675 out of

TABLE 3. Testing result using GoogLeNet architecture

| Class | Classification True | Dataset size | Accuracy (%) |
|------------|---------------------|--------------|--------------|
| Glioma | 157 | 170 | 92 |
| Notumor | 201 | 203 | 99 |
| Meningioma | 166 | 174 | 95 |
| Pituitary | 151 | 156 | 97 |

703 test images being correctly classified into their respective classes. However, 28 images, accounting for 4% of the total test data, are still misclassified.

The obtained confusion matrix results from the dataset testing can be processed to evaluate the model's performance in correctly identifying specific classes by determining the values of Precision (P), Recall (R), and F1-Score (F1S). Here is Table 4 displaying the results obtained from the confusion matrix.

Based on Table 4, the obtained precision values are 0.98 for the AlexNet architecture and 0.96 for the GoogLeNet architecture. The "notumor" class achieves an excellent precision score as it obtains a value of 1.0 in both algorithms. This indicates that the algorithms can effectively identify images with and without tumors. Meanwhile, the Recall value for the AlexNet algorithm is 0.98, which is better than the GoogLeNet value of 0.96. F1-Score is calculated from the Precision and Recall values, where it represents the harmonic mean of precision and recall. It indicates the balance between correctly identifying positive results and the proportion of false negatives. The obtained F1-Score values are 0.98 for the AlexNet architecture and 0.96 for the GoogLeNet architecture. The F1-Score values obtained for both architectures indicate that the classification models have good precision and recall.

This research shows that the use of appropriate input images greatly influences the accuracy in classifying medical images of brain tumors. Apart from that, this research also succeeded in reducing the computational load when training the model because the image size has been changed to be smaller.

3. 2. Discussion This study was conducted to test the architectures used in classifying brain images into four classes with a dataset of 7023 images. The highest accuracy was obtained for the "notumor" class, both using the AlexNet and GoogLeNet architectures. Meanwhile, the lowest accuracy was obtained for the glioma class, with 94% accuracy for the AlexNet architecture and 92% accuracy for the GoogLeNet architecture.

The results obtained in this study showed an accuracy of 98% for the AlexNet architecture and 96% for the GoogLeNet architecture. These accuracy percentages can

TABLE 4. Processed results of confusion matrix

| Class | AlexNet | | | GoogLeNet | | |
|------------|---------|------|------|-----------|------|------|
| | P | R | F | P | R | F |
| Glioma | 0.98 | 0.95 | 0.96 | 0.98 | 0.92 | 0.95 |
| Notumor | 0.32 | 0.87 | 110 | 0.85 | 0.63 | 148 |
| Meningioma | 0.37 | 0.84 | 109 | 0.61 | 0.71 | 148 |
| pituitary | 0.56 | 0.78 | 121 | 0.47 | 0.81 | 146 |

be categorized as very high compared to previous studies on brain tumor classification using CNN architectures. Table 5 presents the accuracy results obtained in previous research using brain tumor images.

Based on Table 5, it can be observed that the previous research achieved the highest accuracy of 94.2%. This result is lower than the accuracy obtained in this study, both using the AlexNet and GoogLeNet architectures. Table 5 shows that from 2018, research related to brain image classification using CNN achieved an accuracy of 91.9%. In the following year, there was an improvement in accuracy with the same research achieving 93.68%. Similarly, from 2019 to 2020, the accuracy reached 94%.

This research achieved a higher accuracy compared to previous studies, demonstrating that it can improve upon previous results using the same images and methodology. This improvement can be attributed to several factors. Firstly, the dataset used in this research consists of 7,023 brain images, while the previous study utilized only 3,064 images. The larger dataset allows for a more comprehensive training of the model and can lead to better accuracy. Another factor contributing to the increased accuracy is the use of the same architecture, CNN, as in the previous study. However, in this research, the CNN architecture was enhanced by incorporating additional feature extraction stages that differ from the previous study. Feature extraction plays a crucial role in improving accuracy, as more filters used in the process result in more feature maps generated. Additionally, employing multiple convolutional stages generates a greater number of image models, which serve as the basis for classification in the fully connected layer.

TABLE 5. Comparison with some previous studies

| Author | Year | Dataset Size | Accuracy (%) |
|-------------------------|------|--------------|--------------|
| Ismael and Qader (30) | 2018 | 3064 | 91.9 |
| Pashaei et al. (23) | 2018 | 3064 | 93.68 |
| Anaraki et al. (31) | 2019 | 600 | 94 |
| Baranwal et al. (32) | 2020 | 3064 | 94 |
| Our Studies (AlexNet) | 2023 | 7023 | 98 |
| Our Studies (GoogLeNet) | 2023 | 7023 | 96 |

4. CONCLUSION

This research succeeded in increasing the classification accuracy of medical images of brain tumors by utilizing the AlexNet and GoogLeNet architectures. Both architectures make changes to the input image using a size of 150x150. This size is much smaller than the original size of the input image in AlexNet and GoogLeNet. However, the input image has been proven

to increase accuracy and be able to speed up the computing process due to its smaller size. The AlexNet architecture achieved higher accuracy compared to the GoogLeNet architecture. Both architectures demonstrated higher accuracy compared to several previous studies. These results suggest that the AlexNet and GoogLeNet architectures in CNN can improve the accuracy percentage for brain tumor image classification. Based on these findings, the AlexNet and GoogLeNet architectures can diagnose brain tumor diseases based on MRI images. The accuracy obtained in the "notumor" class using the AlexNet algorithm was able to identify all the datasets that did not have brain tumor diseases. Patients with brain images from MRI scans can be diagnosed without having to consult a doctor, reducing the cost of expensive consultations. Additionally, this diagnosis can be conducted rapidly without waiting for laboratory examinations such as biopsy, which can take 10 to 15 days.

We hope that in future research, there will be ways to further increase the accuracy compared to this study, to minimize errors in diagnosing brain tumor diseases using machine learning. This would ensure that patients receive prompt and accurate treatment.

5. ACKNOWLEDGMENTS

This work is supported by the Ministry of Education, Culture, Research, and Technology of the Republic of Indonesia based on Contract number: 181/E5/PG.02.00.PL/2023. The authors also gratefully acknowledge the helpful comments and suggestions of the reviewers, which have improved the presentation.

6. REFERENCES

- Nawaz SA, Khan DM, Qadri S. Brain tumor classification based on hybrid optimized multi-features analysis using magnetic resonance imaging dataset. *Applied Artificial Intelligence*. 2022;36(1):2031824. 10.1080/08839514.2022.2031824
- Nanda SJ, Gulati I, Chauhan R, Modi R, Dhaked U. A K-means-galactic swarm optimization-based clustering algorithm with Otsu's entropy for brain tumor detection. *Applied Artificial Intelligence*. 2019;33(2):152-70. 10.1080/08839514.2018.1530869
- Angeli S, Emblem KE, Due-Tonnessen P, Stylianopoulos T. Towards patient-specific modeling of brain tumor growth and formation of secondary nodes guided by DTI-MRI. *NeuroImage: Clinical*. 2018;20:664-73. 10.1016/j.nicl.2018.08.032
- Miller KD, Ostrom QT, Kruchko C, Patil N, Tihan T, Cioffi G, et al. Brain and other central nervous system tumor statistics, 2021. *CA: a cancer journal for clinicians*. 2021;71(5):381-406. 10.3322/caac.21693
- Le D-N, Parvathy VS, Gupta D, Khanna A, Rodrigues JJ, Shankar K. IoT enabled depthwise separable convolution neural network with deep support vector machine for COVID-19 diagnosis and classification. *International journal of machine learning and cybernetics*. 2021:1-14. 10.1007/s13042-020-01248-7
- Hamghalam M, Wang T, Lei B. High tissue contrast image synthesis via multistage attention-GAN: application to segmenting brain MR scans. *Neural Networks*. 2020;132:43-52. 10.1016/j.neunet.2020.08.014
- Arunachalam S, Sethumathavan G. An effective tumor detection in MR brain images based on deep CNN approach: i-YOLOV5. *Applied Artificial Intelligence*. 2022;36(1):2151180. 10.1080/08839514.2022.2151180
- Badr CE, Silver DJ, Siebzehnrubel FA, Deleyrolle LP. Metabolic heterogeneity and adaptability in brain tumors. *Cellular and Molecular Life Sciences*. 2020;77:5101-19. 10.1007/s00018-020-03569-w
- Qu Z, Cao C, Liu L, Zhou D-Y. A deeply supervised convolutional neural network for pavement crack detection with multiscale feature fusion. *IEEE transactions on neural networks and learning systems*. 2021;33(9):4890-9. 10.1109/TNNLS.2021.3062070
- Amjoud AB, Amrouch M. Object Detection Using Deep Learning, CNNs and Vision Transformers: A Review. *IEEE Access*. 2023. 10.1109/ACCESS.2023.3266093
- Chahal PK, Pandey S, Goel S. A survey on brain tumor detection techniques for MR images. *Multimedia Tools and Applications*. 2020;79:21771-814. 10.1007/s11042-020-08898-3
- Takahashi M, Miki S, Fujimoto K, Fukuoka K, Matsushita Y, Maida Y, et al. Eribulin penetrates brain tumor tissue and prolongs survival of mice harboring intracerebral glioblastoma xenografts. *Cancer Science*. 2019;110(7):2247-57. 10.1111/cas.14067
- Li Q, Liu X, He Y, Li D, Xue J. Temperature guided network for 3D joint segmentation of the pancreas and tumors. *Neural Networks*. 2023;157:387-403. 10.1016/j.neunet.2022.10.026
- Zohrevand A, Imani Z. Holistic persian handwritten word recognition using convolutional neural network. *International Journal of Engineering*. 2021;34(8):2028-37. 10.5829/ije.2021.34.08b.24
- Siddique MAB, Arif RB, Khan MMR, editors. Digital image segmentation in matlab: A brief study on otsu's image thresholding. 2018 international conference on innovation in engineering and technology (ICIET); 2018: IEEE. 10.1109/CIET.2018.8660942
- Mulyadi R, Islam AA, Murtala B, Tammase J, Hatta M, Firdaus M. Diagnostic yield of the combined Magnetic Resonance Imaging and Magnetic Resonance Spectroscopy to predict malignant brain tumor. *bmj*. 2020;9:1486. 10.15562/bmj.v9i1.1486
- Isaieva K, Laprie Y, Turpault N, Houssard A, Felblinger J, Vuissoz P-A. Automatic tongue delineation from mri images with a convolutional neural network approach. *Applied Artificial Intelligence*. 2020;34(14):1115-23. 10.1080/08839514.2020.1824090
- Shamrat FJM, Azam S, Karim A, Ahmed K, Bui FM, De Boer F. High-precision multiclass classification of lung disease through customized MobileNetV2 from chest X-ray images. *Computers in Biology and Medicine*. 2023;155:106646. 10.1016/j.compbiomed.2023.106646
- Nawaz A, Rehman AU, Ali TM, Hayat Z, Rahim A, Uz Zaman UK, et al. A Comprehensive Literature Review of Application of Artificial Intelligence in Functional Magnetic Resonance Imaging for Disease Diagnosis. *Applied Artificial Intelligence*. 2021;35(15):1420-38. 10.1080/08839514.2021.1982185
- Khan AI, Wani MA. Patch-based segmentation of latent fingerprint images using convolutional neural network. *Applied*

- Artificial Intelligence. 2019;33(1):87-100. 10.1080/08839514.2018.1526704
21. Zhao X, Wu Y, Song G, Li Z, Zhang Y, Fan Y. A deep learning model integrating FCNNs and CRFs for brain tumor segmentation. *Medical image analysis*. 2018;43:98-111. 10.1016/j.media.2017.10.002
 22. Li Z, Liu F, Yang W, Peng S, Zhou J. A survey of convolutional neural networks: analysis, applications, and prospects. *IEEE transactions on neural networks and learning systems*. 2021. 10.1109/TNNLS.2021.3084827
 23. Pashaei A, Sajedi H, Jazayeri N, editors. Brain tumor classification via convolutional neural network and extreme learning machines. 2018 8th International conference on computer and knowledge engineering (ICCKE); 2018: IEEE. 10.1109/ICCKE.2018.8566571
 24. Oyewola DO, Dada EG, Misra S, Damaševičius R. A novel data augmentation convolutional neural network for detecting malaria parasite in blood smear images. *Applied Artificial Intelligence*. 2022;36(1):2033473. 10.1080/08839514.2022.2033473
 25. Niepceron B, Nait-Sidi-Moh A, Grassia F. Moving medical image analysis to GPU embedded systems: Application to brain tumor segmentation. *Applied Artificial Intelligence*. 2020;34(12):866-79. 10.1080/08839514.2020.1787678
 26. Billah ME, Javed F. Bayesian convolutional neural network-based models for diagnosis of blood cancer. *Applied Artificial Intelligence*. 2022;36(1):2011688. 10.1080/08839514.2021.2011688
 27. Rohani M, Farsi H, Mohamadzadeh S. Deep Multi-task Convolutional Neural Networks for Efficient Classification of Face Attributes. *International Journal of Engineering, Transactions B: Applications*. 2023;36(11):2102-11. 10.5829/ije.2023.36.11b.14
 28. Arabahmadi M, Farahbakhsh R, Rezazadeh J. Deep learning for smart Healthcare—A survey on brain tumor detection from medical imaging. *Sensors*. 2022;22(5):1960. <https://doi.org/10.3390/s22051960>
 29. Xie Y, Zaccagna F, Rundo L, Testa C, Agati R, Lodi R, et al. Convolutional neural network techniques for brain tumor classification (from 2015 to 2022): Review, challenges, and future perspectives. *Diagnostics*. 2022;12(8):1850. 10.3390/diagnostics12081850
 30. Ismael MR, Abdel-Qader I, editors. Brain tumor classification via statistical features and back-propagation neural network. 2018 IEEE international conference on electro/information technology (EIT); 2018: IEEE. 10.1109/EIT.2018.8500308
 31. Anaraki AK, Ayati M, Kazemi F. Magnetic resonance imaging-based brain tumor grades classification and grading via convolutional neural networks and genetic algorithms. *biocybernetics and biomedical engineering*. 2019;39(1):63-74. 10.1016/j.bbe.2018.10.004
 32. Baranwal SK, Jaiswal K, Vaibhav K, Kumar A, Srikantaswamy R, editors. Performance analysis of brain tumour image classification using CNN and SVM. 2020 Second International Conference on Inventive Research in Computing Applications (ICIRCA); 2020: IEEE. 10.1109/ICIRCA48905.2020.9183023
 33. Deepak S, Ameer P. Brain tumor classification using deep CNN features via transfer learning. *Computers in biology and medicine*. 2019;111:103345. 10.1016/j.compbiomed.2019.103345
 34. Daniel MC, Ruxandra LM, editors. Brain Tumor Classification Using Pretrained Convolutional Neural Networks. 2021 16th International Conference on Engineering of Modern Electric Systems (EMES); 2021: IEEE. 10.1109/EMES52337.2021.9484102
 35. Emadi M, Jafarian Dehkordi Z, Iranpour Mobarakeh M. Improving the accuracy of brain tumor identification in magnetic resonance using super-pixel and fast primal dual algorithm. *International Journal of Engineering, Transactions A Basics*.. 2023;36(3):505-12. 10.5829/ije.2023.36.03c.10
 36. Rehman A, Naz S, Razzak MI, Akram F, Imran M. A deep learning-based framework for automatic brain tumors classification using transfer learning. *Circuits, Systems, and Signal Processing*. 2020;39:757-75. 10.1007/s00034-019-01246-3
 37. Alem A, Kumar S. End-to-End Convolutional Neural Network Feature Extraction for Remote Sensed Images Classification. *Applied Artificial Intelligence*. 2022;36(1):2137650. 10.1080/08839514.2022.2137650
 38. M. Alqhtani S. BreastCNN: a novel layer-based convolutional neural network for breast cancer diagnosis in DMR-thermogram images. *Applied Artificial Intelligence*. 2022;36(1):2067631. 10.1080/08839514.2022.2067631
 39. Agrawal R, Sharma M, Singh BK. Performance evaluation of automated brain tumor detection systems with expert delineations and interobserver variability analysis in diseased patients on magnetic resonance imaging. *Applied Artificial Intelligence*. 2018;32(7-8):670-91. 10.1080/08839514.2018.1504500
 40. Hasan MM, Ali H, Hossain MF, Abujar S, editors. Preprocessing of continuous bengali speech for feature extraction. 2020 11th International Conference on Computing, Communication and Networking Technologies (ICCCNT); 2020: IEEE. 10.1109/ICCCNT49239.2020.9225469
 41. Pitak L, Saengprachatanarug K, Laloon K, Posom J. Predicting the true density of commercial biomass pellets using near-infrared hyperspectral imaging. *Artificial Intelligence in Agriculture*. 2022;6:266-75. 10.1016/j.aiaa.2022.11.004
 42. Alamri NMH, Packianather M, Bigot S. Deep learning: Parameter optimization using proposed novel hybrid bees Bayesian convolutional neural network. *Applied Artificial Intelligence*. 2022;36(1):2031815. 10.1080/08839514.2022.2031815
 43. Augusto Costa J, Carmona Cortes O. A Convolutional Neural Network for Detecting Faults in Power Distribution Networks along a Railway: A Case Study Using YOLO. *Applied Artificial Intelligence*. 2021;35(15):2067-86. 10.1080/08839514.2021.1998974
 44. Alzughabi S, El Khediri S. A Cloud Intrusion Detection Systems Based on DNN Using Backpropagation and PSO on the CSE-CIC-IDS2018 Dataset. *Applied Sciences*. 2023;13(4):2276. 10.3390/app13042276
 45. Tri Handoyo A, Kusuma GP. Severity Classification of Diabetic Retinopathy Using Ensemble Stacking Method. *Revue d'Intelligence Artificielle*. 2022;36(6). 10.18280/ria.360608

COPYRIGHTS

©2024 The author(s). This is an open access article distributed under the terms of the Creative Commons Attribution (CC BY 4.0), which permits unrestricted use, distribution, and reproduction in any medium, as long as the original authors and source are cited. No permission is required from the authors or the publishers.



Persian Abstract

چکیده

تومورهای مغزی یکی از کشنده ترین بیماری ها در جهان هستند. این بیماری می تواند هر فردی را بدون در نظر گرفتن جنسیت یا گروه های سنی خاص مورد حمله قرار دهد. تشخیص تومورهای مغزی با شناسایی دستی تصاویر حاصل از اسکن توموگرافی کامپیوتری یا تصویربرداری تشدید مغناطیسی انجام می شود و امکان بروز خطاهای تشخیصی را فراهم می کند. علاوه بر این، تشخیص را می توان با استفاده از تکنیک های بیوپسی انجام داد. این تکنیک بسیار دقیق است، اما زمان زیادی طول می کشد، حدود 10 تا 15 روز و شامل تجهیزات و پرسنل پزشکی زیادی است. بر این اساس، فناوری یادگیری ماشینی مورد نیاز است که بتواند بر اساس تصاویر تولید شده از MRI طبقه بندی کند. هدف این تحقیق افزایش دقت تحقیقات قبلی در طبقه بندی تومورهای مغزی است تا در تشخیص تومورهای مغزی خطا رخ ندهد. روش مورد استفاده در این تحقیق شبکه عصبی کانولوشن با استفاده از معماری AlexNet و GoogLeNet است. نتایج این تحقیق برای معماری AlexNet 98% و برای GoogLeNet 96% به دست آورد. این نتیجه در مقایسه با تحقیقات قبلی بیشتر است. این یافته می تواند بار محاسباتی را در طول آموزش مدل کاهش دهد. نتایج این تحقیق می تواند به پزشکان در تشخیص سریع و دقیق تومورهای مغزی کمک کند.
